Characterization of beech milled wood lignin by pyrolysis- gas chromatography-photoionization mass spectrometry. Anal Chem 59: 508-512

ARTICLE *in* ANALYTICAL CHEMISTRY · FEBRUARY 1987

Impact Factor: 5.64 · DOI: 10.1021/ac00130a029

3 AUTHORS:

Wim Genuit
Shell Global
17 PUBLICATIONS **357** CITATIONS
SEE PROFILE

Jaap J. Boon
JAAP Enterprise for Art Scientific Studies, Am…
332 PUBLICATIONS **8,296** CITATIONS
SEE PROFILE

O. Faix
University of Hamburg
207 PUBLICATIONS **5,029** CITATIONS
SEE PROFILE

without any interferring substances.

When the sample contains several mutagens, the determination of the individual constituents is more questionable. A preseparation is then recommended.

ACKNOWLEDGMENT

We are grateful to Maurice Hofnung, Institut Pasteur, Paris, for providing the bacterial strain and to Ján Garaj, Slovak Technical University, Bratislava, for stimulating support of this work.

Registry No. 1, 6281-23-8; 2, 1874-24-4; 3, 1874-12-0; 4, 90147-18-5; 5, 90147-21-0; 6, 90147-19-6; 7, 710-25-8; 8, 14308-65-7; 9, 804-36-4; 10, 67-20-9.

LITERATURE CITED

(1) Fishbein, L. *Potential Industrial Carcinogens and Mutagens*; Amsterdam, Oxford, New York, 1979; Vol. 4.
(2) Groenen, P. J.; de Cook-Bethbeder, M. W.; Bouwman, J.; Dhont, J. H. "*N-Nitroso Compounds: Analysis, Formation and Occurrence*; Walker, E. A., Griciute, L., Castegnaro, M., Börzsönyi, M., Eds.; Lyon, 1980.
(3) Maron, D. M.; Ames, B. N. *Mutat. Res.* **1983**, *113*, 173-215.
(4) Quillardet, Ph.; Huisman, O.; D'Ari, R.; Hofnung, M. *Proc. Natl. Acad. Sci. U.S.A.* **1982**, 5971-5975.
(5) Quillardet, Ph.; Hofnung, M. *Mutat. Res.* **1985**, *147*, 65-78.
(6) Quillardet, Ph.; de Belcombe, Ch.; Hofnung, M. *Mutat. Res.* **1985**, *147*, 79-95.
(7) Hayes, S.; Gordon, A.; Sadowski, I.; Hayes, C. *Mutat. Res.* **1984**, *130*, 97-106.
(8) Karube, I.; Nakahara, T.; Matsunaga, T.; Shuichi, S. *Anal. Chem.* **1982**, *54*, 1725-1727.
(9) Hofnung, M., special publication, Institute Pasteur, Paris, 1982.
(10) McCalla, D. R. *Environ. Mutagen.* **1983**, *5*, 745-765.
(11) Atkinson, R. L. *Nutr. Rep. Int.* **1971**, *3*, 363-367.
(12) Farkaš, J. *Chem. Abstr.* **1976**, *84*, 119900.
(13) Kellová, G.; Šturdík, E.; Štibránvi, L.; Drobnica, Ľ.; Augustín, J. *Folia Microbiol. (Prague)* **1984**, *29*, 23-34.
(14) Šturdík, E.; Rosenberg, M.; Štibránvi, L.; Baláž, Š.; Chreňo, O.; Ebringer, L.; Ilavský, D.; Végh, D. *Chem.-Biol. Interact.* **1985**, *53*, 145-153.
(15) Miller, J. H. *Experiments in Molecular Genetics*; Cold Spring Harbor Laboratory: Cold Spring Harbor, NY, 1972.
(16) Eckschlager, K.; Štěpánek, V. *Information Theory as Applied to Chemical Analysis*; Wiley-Interscience: New York, 1979.
(17) Kaiser, H.; Menzies, A. C. *The Limit of Detection of a Complete Analytical Procedure*; Adam Hilger: London, 1968.
(18) Borgatzi, A. R.; Tarozzi, F.; Grisetig, G.; Brusco, A. *Nuova Vet.* **1970**, *46*, 6-21.

RECEIVED for review April 14, 1986. Accepted September 23, 1986.

Characterization of Beech Milled Wood Lignin by Pyrolysis–Gas Chromatography–Photoionization Mass Spectrometry

Wim Genuit[1] and Jaap J. Boon*

Mass Spectrometry of Macromolecular Systems Unit, FOM-Institute for Atomic and Molecular Physics, Kruislaan 407, 1098 SJ Amsterdam, The Netherlands

Oskar Faix

Bundesforschungsanstalt für Forst- und Holzwirtschaft, Institut für Holzchemie und chemische Technologie des Holzes, Leuschnerstrasse 91, 2050 Hamburg 80, West Germany

A Curie-point pyrolysis–gas chromatography–photoionization mass spectrometry instrument has been used for characterization of beech milled wood lignin. The light source for photoionization is a rare gas resonance lamp. The main pyrolysis products have been identified and are fitted into a proposed thermal degradation scheme for the beech lignin. It is shown that the responses for these products depend strongly on ionizing energy. The cumulative photoionization mass spectra at two photon energies, 11.8 eV (Ar I) and 10.6 eV (Kr I), are compared to a 15-eV electron impact pyrolysis mass spectrum. The Ar I photoionization and 15-eV electron impact ionization mass spectra both show a high abundance of fragment ions, whereas in the Kr I mass spectrum predominantly molecular ion peaks are observed.

Curie-point pyrolysis is a useful general method for thermal depolymerization of macromolecular materials, producing characteristic chemical units amenable to gas chromatographic or mass spectrometric analysis (*1*, *2*). A large variety of materials has been characterized by automated Curie-point pyrolysis–mass spectrometry (Py–MS) (*2*), and many groups of biomaterials have been differentiated by subjecting their Py–MS fingerprints to advanced numerical data analysis methods (*2–6*).

However, mass spectrometric results on the composition of pyrolysates depend strongly on the way in which the pyrolysate is transferred from the pyrolysis zone to the ion source and on the ionization conditions (*6–9*). The transfer problem can be avoided by applying in-source pyrolysis, but this in turn leads to rapid source contamination and sets and undesirable restriction to the heating rate, to prevent high-pressure pulses in the vacuum system. In the instrument described here a chromatographic inlet is used, which provides well-defined transfer conditions. Furthermore, this method enables the identification of individual pyrolysis products (Py–GC–MS mode), as well as the production, by spectrum accumulation, of a useful mass spectral fingerprint (Py–MS mode).

Py–MS studies (*2*) generally apply low-energy (10–16 eV) electron impact ionization (EI) to enhance the characteristics of the mass spectral fingerprints by reducing fragmentation compared to 70-eV EI. At these low energies, however, small variations in electron energy lead to large differences in mass spectra, which is one of the main factors involved in poor interlaboratory reproducibility in Py–MS (*8*). Photoionization (PI) by means of a vacuum-UV light source is an attractive alternative to low-energy EI, because of the well-defined, highly constant, and reproducible ionizing energy. Although the ion yield of PI is much lower than that of 70-eV EI, it can be expected to be equal to or larger than that of EI at energies near threshold, because photoionization cross sections have

[1] Present address: Shell Research Laboratory, Badhuisweg 3, 1031 CM Amsterdam, The Netherlands.

0003-2700/87/0359-0508$01.50/0

a much steeper onset at threshold than EI cross sections (*10*). Our vacuum-UV light source allows a choice of gas for emission. In this paper the differences in response between Ar I and Kr I photon as ionization media for the characterization of phenolic compounds evolved in the pyrolysis of lignin are explored.

The technique of gas chromatography–photoionization mass spectrometry (GC–PIMS) as such has been demonstrated before by Washida et al., who investigated the fragmentation behavior of some organic compounds (*11*, *12*). Their instrument had a lower sensitivity than the one described here, presumably owing to a weaker lamp intensity and a lower ion source pressure. Genuit and Boon (*9*) have reported earlier on the results of the characterization of the glucose polymer amylose by pyrolysis GC–PIMS. In this paper, the utility of our pyrolysis–gas chromatography–photoionization mass spectrometry (Py–GC–PIMS) instrument is demonstrated by the characterization of a hard wood "milled wood lignin", which is a mainly ether-linked polyphenolic polymer in plant cell walls.

Lignin is an essential component of the woody stems of arborescent gymnosperms and angiosperms which makes up 19–28% of the total wood. Lignin also forms an integral part of all vascular plants, including the herbaceous varieties. The formation of lignin proceeds via an enzyme-initiated dehydrogenative polymerization of three primary precursors: *trans*-coniferyl, *trans*-sinapyl, and *trans*-*p*-coumaryl alcohols (*13*). During biosynthesis, these precursors undergo structural changes due to coupling processes, displacements, and addition and subtraction reactions. The polymerization gives rise to at least 10 types of intermonomeric linkages.

In the study of the structure of lignin, the isolation and purification of lignin from the plant tissue without altering its structure are very difficult. Further, chemical degradation methods have to be applied to depolymerize the lignin, and the structure of degradation products must be elucidated. Besides chemical degradation studies, information on lignin structure can be obtained by spectroscopic methods: ultraviolet and infrared spectroscopy and ^{1}H and ^{13}C NMR. Some attempts have been made to unify all available information into a structural scheme of lignin (*14–16*).

For lignin classification, frequently degradation methods are applied to determine the abundance of H (*p*-hydroxyphenyl), G (guaiacyl or 3-methoxy-4-hydroxyphenyl), and S (syringyl or 3,5-dimethoxy-4-hydroxyphenol) monomers in the degradation mixture. The lignins are classified according to their H/G and G/S ratios. Classical degradation methods are very time-consuming: the performance of these methods typically takes several days. In this respect, pyrolysis as a high-energy degradation method is a promising, rapid method for characterization of lignins. Earlier Py–GC (*17*) and Py–MS (*18*, *19*) have been used for classification of different lignin types. Py–GC–MS has been applied to identify the pyrolysis products of several lignins and lignin-containing materials (*20–22*). For the Py–GC–PIMS study described here, a beech milled wood sample was taken for analysis, because the structure of beech lignin is well investigated (*16*) and consists mainly of G (guaiacyl) and S (syringyl) units.

EXPERIMENTAL SECTION

A scheme of the instrument is shown in Figure 1. The main parts will be described briefly below.

Pyrolysis Unit and Gas Chromatograph. A Varian Aerograph Series 1400 gas chromatograph was modified for our purposes. The septum inlet was exchanged for a newly designed internally heatable Curie-point pyrolysis unit (FOM-3LX), suitable for pyrolysis on-line with fused-silica capillary columns (*23*). In this pyrolysis unit, a glass liner around a ferromagnetic wire coated with the sample is placed on a Kalrez interface directly above the entrance of the capillary column. The glass liner is surrounded by a ceramic tube kept at 160 °C, which in turn is surrounded by a high frequency coil. The unit is flushed with oxygen-free nitrogen which was also used as the carrier gas.

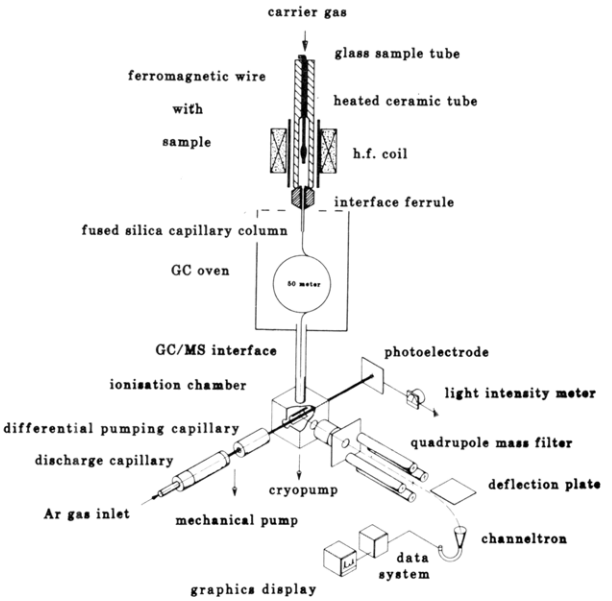

Figure 1. Schematic overview of the pyrolysis–gas chromatograph–photoionization mass spectrometry instrument, which consists of a Curie-point pyrolysis unit (FOM-3LX), a gas chromatograph equipped with a fused-silica capillary column, a direct coupling interface probe to the ion source, a photoionization mass spectrometer, and a data system.

The GC oven was equipped with a 30-m fused-silica capillary column (320 μm i.d.) with a 1.0 μm thick chemically bonded Durabond DB-1 coating (J&W Scientific, Rancho Cordova, CA). Nitrogen was used as the carrier gas. The column inlet pressure is 0.6 bar. The average gas velocity is 65 cm/s when the oven is at room temperature. The column inlet is heated to 180 °C.

During pyrolysis injection, the oven was at room temperature to trap the pyrolysate in the first few centimetres of the column. After injection the oven was first heated rapidly to 80 °C and then programmed from 80 to 100 °C at 2 °C/min and from 100 °C at 6 °C/min.

Interface and Mass Spectrometer. The capillary column is fed from the oven to the mass spectrometer through a resistively heated stainless steel capillary. The column outlet is coupled directly to the ion source via a sliding probe (Vacumetrics, USA). The interface capillary and probe are heated to 280 °C.

The photoionization mass spectrometer has previously been described in detail (*24*). Briefly, it consists of a windowless, differentially pumped, glow discharge resonance lamp, a small ionization chamber, and a Balzers QMG 511 quadrupole mass filter. Argon and krypton are used as discharge gases, producing photon energies of 11.6 and 11.8 eV and 10.0 and 10.6 eV, respectively. The ionization chamber allows for the high sample gas density in the ionization region that is needed to obtain a sufficiently high ion yield. The ion source is heated to 100 °C to prevent memory effects due to adsorption of high-boiling compounds. The quadrupole is scanned from 30 to 235 amu at a rate of 1 scan/s. The ions are detected by a dynode multiplier in the counting mode. The vacuum chamber is pumped by a 1000 L/s cryopump (Varian VK-12). The pressure inside the ion source is about 10^{-2} torr (Baratron capacitance manometer measurement) and in the vacuum chamber about 10^{-5} torr.

Data System. Data aquisition and quadrupole scan control are performed by a Camac data system. The Camac system is controlled by a LSI 11/23 microcomputer. The mass spectra are stored on a 20 Mbyte Winchester disk. The data analysis software enables scanning of the mass–time data matrix in two dimensions, constructing either total ion current and mass chromatograms or single or cumulative mass spectra (spectra summed in time). Noise reduction is accomplished by setting a discrimination level of two counts for each spectrum channel, thus rejecting all single counts.

Py-EI-MS, Py-GC-EI-MS, and Py-FID Gas Chromatography. The 15-eV electron impact pyrolysis mass spectrum was produced by the FOM-autopyms, an automated Curie-point pyrolysis mass spectrometer system described elsewhere (*6*). A modification was made with respect to the pyrolysis chamber, which was heated to prevent condensation of high-boiling compounds.

The Py-GC-EI-MS data were obtained with a Packard 438S gas chromatograph, equipped with the same type of pyrolysis unit and column as mentioned above, coupled to a Jeol JMS-DX300 double focusing mass spectrometer. Mass spectra were obtained at 70 eV.

The FID chromatogram was made on a Carlo Erba 4200 gas chromatograph, equipped with the same type of pyrolysis unit, the same column as mentioned above, and a flame ionization detector. Helium served as the carrier gas. Temperature programming was the same as in the Py-GC-PIMS setup. Data were processed by a gas chromatographic data system (Nelson Analytical 4400). The time scale was calibrated on the retention times of the *n*-alkanes C_{12}–C_{23}, which were measured in a separate GC run with the same temperature program, in order to determine retention indices.

Reagents. The milled wood lignin (MWL) sample was prepared from beech wood according to Björkman (*25*) with the following modifications: a planetary ball mill was used instead of a vibratory ball mill. Milling was carried out in a nitrogen atmosphere and milling time was 160 h. The subsequent purification procedure is described by Schweers and Faix (*26*). The sample was suspended in water at a concentration of 1 mg/mL. A small droplet of this suspension (5 μL) was put on a ferromagnetic wire for pyrolysis analysis (Curie point 610 °C) and dried in vacuo.

RESULTS AND DISCUSSION

Cumulative Spectra. Figure 2 shows two cumulative spectra of the beech MWL pyrolysate, obtained by summing all spectra (1–2000) from the GC-MS run with Ar I (middle) and Kr I (bottom) photoionization, respectively. For comparison a 15-eV EI pyrolysis mass spectrum, as obtained from the FOM-autopyms system, is shown on top.

In the Ar I spectrum, mass 40 is due to an $Ar^{\bullet+}$ background produced by residual higher resonance lines in the lamp output, as well as by photoelectrons that are accelerated in the extraction field of the ion source. For the same reason in the Kr spectrum the peaks at masses 82 to 86, corresponding to mostly $Kr^{\bullet+}$ ions, should be disregarded. In both spectra part of the mass 42 signal arises from nitrogen ion/molecule reactions leading to the N_3^+ ion. In the Ar I spectrum and the 15-eV EI spectrum the same masses occur in the range 100–220, whereas in the Kr I spectrum some of these masses (i.e., 181, 167, 151, 137, 109) are missing. These uneven-numbered masses corresponded to fragment ions, as becomes clear when the Ar I GC-MS data file is studied.

In the EI spectrum, the ion yield in the higher mass range is markedly increased, compared to the situation in which the pyrolysis chamber is not heated (cf. spectrum E.9 in ref 2). Apparently a significant part of the high-boiling pyrolysate fraction condenses in the glass liner around the Curie-point wire, when the pyrolysis chamber is kept at room temperature.

Identification and Significance of the Pyrolysis Products. Figure 3 shows three total ion chromatograms, produced by a flame ionization detector (FID) and Ar I and Kr I photoionization, respectively. In order to eliminate the $Ar^{\bullet+}$ and N_3^+ background the mass range 30–45 is rejected in the Ar I chromatogram. The separation in the two PI chromatograms is only slightly less than in the FID case, indicating that the use of nitrogen instead of helium and the column outlet being at vacuum are not detrimental to the chromatographic resolution (*27*).

In Table I the identified pyrolysis products are given, together with their molecular weights, the most abundant fragment ions in the Ar I spectrum, the responses of the three

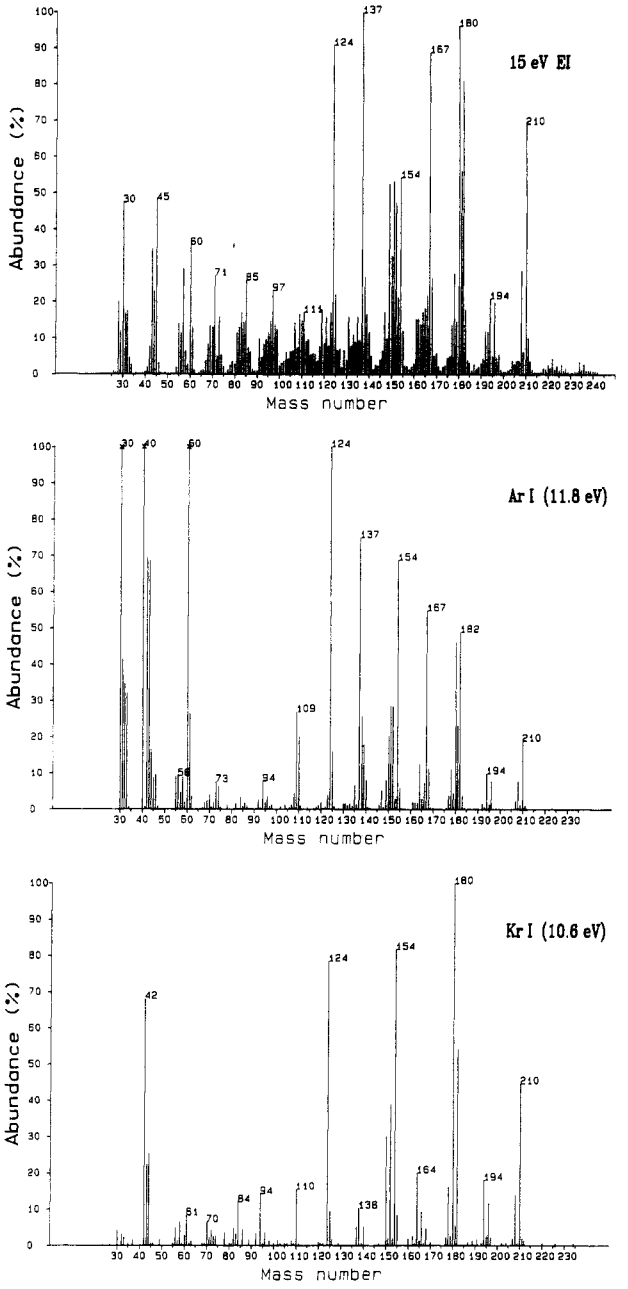

Figure 2. Electron impact Py-MS (15 eV) spectrum (top), cumulative Ar I (11.8 eV) photoionization mass spectrum (middle), and cumulative Kr I (10.6 eV) photoionization mass spectrum (bottom) of the Curie-point (610 °C) pyrolysate of beech MWL.

detectors (normalized on total chromatogram area), and the retention times relative to those of the C_{12}–C_{23} *n*-alkanes, as measured on the Py-GC system. Tentative identifications are indicated with a question mark. The identity of the other compounds was confirmed by comparison with capillary GC high-resolution MS data (*23*). The highly volatile pyrolysate fraction is not included in Table I, since it consists mainly of nonspecific products such as formaldehyde and acetic acid. The high-boiling components are all guaiacyl (G) or syringyl (S) derivatives.

A number of these compounds have been reported by Martin et al. (*20*), who studied a similar sample with packed column GC-MS. They, however, found a much higher amount of desmethoxy and guaiacyl compounds, relative to compounds with syringyl units. In Table II the abundance of compounds without, with one, and with two methoxy groups in our FID, 70-eV EI, Ar I and Kr I chromatograms are given. These data may be compared to the syringyl:guaiacyl:phenolic ratio estimated by Nimz (*16*) on the basis of chemical degradation

Table I. Pyrolysis Products of Beech Milled Wood Lignin

peak no.	identification	mol wt	fragment ions (Ar)	% normalized area Ar	Kr	FID	rel retention time (FID)	structure[a]
1	phenol	94		0.9	1.4	0.1		P
2	*o*-methylphenol	108		0.2	0.3	0.1		P-C
3	*p*-methylphenol	108		0.3	0.4	0.1		P-C
4	guaiacol	124	109	7.3	11	4.7		G
5	catechol	110		2.3	1.9	0.5		P-OH
6	guaiacylmethane	138	123	1.0	0.8	0.7		G-C
7	hydroxyguaiacol	140	125	0.9	0.8		12.28	G-OH
8	methylcatechol	124		0.5	0.5		12.28	C-P-OH
9	dihydroxybenzene	110		0.1			12.28	P-OH
10	guaiacylethane	152	137	0.1		0.3	12.45	G-C-C
11	methylcatechol	124		0.3		0.4	12.52	C-P-OH
12	guaiacylethene	150	135	3.5	5.9	4.1	12.82	G-C=C
13	syringol	154	139	8.9	15	9.0	13.09	S
14	3-guaiacylprop-1-ene	164	149	0.5	0.4	1.0	13.28	G-C-C=C
15	guaiacyl aldehyde	152	151	4.7	5.9	2.7	13.52	G-CO
16	*cis*-1-guaiacylprop-1-ene	164	149	0.3	0.4	0.5	13.78	G-C=C-C
17	syringylmethane	168	153	1.2	0.9	1.4	14.07	S-C
18	guaiacylethanal	166	137	2.2	0.5	1.3	14.11	G-C-CO
19	*trans*-1-guaiacylprop-1-ene	164	149	1.7	3.0	2.5	14.18	G-C=C-C
20	guaiacylethanone	166	151	1.9	1.4	1.3	14.42	G-CO-C
21		162	147	0.2		1.7	14.48	G-C_3H_6
22		162	147	0.2	0.6	1.2	14.54	G-C_3H_6
23	1-guaiacylpropan-2-one	180	137	0.4		0.7	14.85	G-C-CO-C
24	syringylethene	180	165	3.3	5.5	7.3	15.24	S-C=C
25	1-guaiacylprop-3-en-1-one	178	151	1.0	0.8	1.4	15.41	G-CO-C=C
26	3-syringylprop-1-ene	194		0.4	0.7	1.7	15.63	S-C-C=C
27	?	180		0.3	0.3	0.3	15.89	
28	syringaldehyde	182	181	6.6	8.8	6.6	16.06	S-CO
29	*cis*-1-syringylprop-1-ene	194		0.1	0.3	1.7	16.11	S-C=C-C
30	*cis*-3-guaiacylprop-2-enol	180	124	1.5	0.7	0.8	16.28	G-C=C-C-OH
31		192	177	0.2		2.5	16.45	S-C_3H_6
32	syringylethanal	196	167	2.6	1.5	3.4	16.50	S-C-C-O
33	*trans*-1-syringylprop-1-ene (trans)	194		1.2	1.9	4.6	16.61	S-C=C-C
34	syringylethanone	196	181	2.3	1.5		16.83	S-CO-C
35	3-guaiacylprop-2-enal	178	147	1.5	1.2		16.83	G-C=C-CO
36	*trans*-3-guaiacylprop-2-enol	180	124	21	13	13	16.92	G-C=C-C-OH
37	1-syringylpropan-2-one	210	167				17.16	S-C-CO-C
	syringic acid	212	181				17.16	S-COO-C
38	1-syringylprop-2-en-1-one	208		0.6	0.7	2.1	17.77	S-CO-C=C
39	3-syringylpropanol	212	168	0.3	0.3	0.4	18.40	S-C-C-C-OH
40	*cis*-3-syringylprop-2-enol	210	167	1.4	0.6	1.2	18.61	S-C=C-C-OH
41	3-syringylprop-2-enal	208	180	1.4	1.8	4.9	19.26	S-C=C-CO
42	*trans*-3-syringylprop-2-enol	210	167	13	8.6	10	19.37	S-C=C-C-OH

[a] Guaiacyl (G) = 3-methoxy-4-hydroxyphenyl; syringyl (S) = 3,5-dimethoxy-4-hydroxyphenyl

Table II. Abundance of Syringyl, Guaiacyl, and Phenol Units in the Pyrolysate of Beech Milled Wood Lignin

	Ar I PI	Kr I PI	70 eV EI	FID	Chem degradation[a]
syringyl	43.5	48.1	62.3	56.8	40
guaiacyl	49.9	46.4	36.3	37.2	56
phenol	4.6	4.5	1.4	1.2–1.8	4

[a] Nimz (*16*).

data: S:G:H = 40:56:4. The Ar I PI results are close to this ratio. The FID and 70-eV EI results are in very good agreement with each other but seem to overestimate the syringyl content in comparison with the ratio determined by Nimz, and with the photoionization data. Anyway, it is clear that pyrolytic dissociation in the FOM-3LX unit does not effect an important loss of methoxy groups from the syringyl or guaiacyl units. This observation is supported by recent Curie-point pyrolysis GC–MS studies (*21*) on a synthetic lignin (DHP) with only methoxylated units. Probably the high abundance of phenolic and guaiacyl units in Martin's results is caused by a much stronger pyrolytic degradation, which leads to demethoxylation of the syringyl and guaiacyl units. Major compounds in Table I are guaiacol, syringol, syringyl–ethene, syringaldehyde, 3-guaiacylprop-2-enol, and 3-syringylprop-2-enol. These compounds should be a reflection of the polymeric structure as proposed by Nimz et al. (*16*). In this structure, about 60% of the intermonomeric linkages are β-0–4 linkages. The lignin contains β-1 linkages between the syringyl units and furthermore phenylpropanoid, phenylcoumaran, and biphenyl elements with either syringyl or guaiacyl units. Thermal activation of the lignin may lead to reduction of the β-0–4 phenolic bonds. Figure 4 proposes thermal activation schemes for the β-1 linkage element and the phenylpropanoid unit. Although several alternative routes may be possible, these schemes explain a number of the major compounds observed in the lignin pyrolysate. The proposed schemes remain to be confirmed by a study of suitable model compounds.

Response Differences. Comparison of the relative chromatogram peak areas obtained with the three detectors (Table I) reveals important differences between the responses at the two photoionization energies and even larger variations between these PI chromatograms and the FID chromatogram. It is not clear whether the latter variations only reflect response differences or whether they are partly due to different pyrolytic conditions. The anomalously high FID signals, compared to the PI signals, in the case of the unidentified C_3H_6-substituted guaiacol and syringol compounds suggest

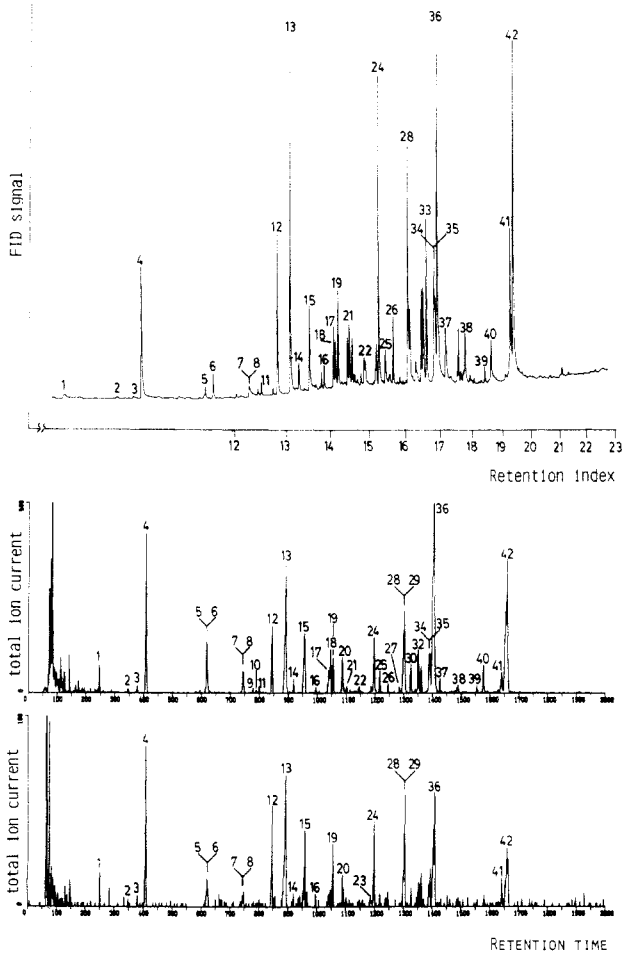

Figure 3. FID chromatogram (top), Ar I total ion chromatogram (middle), and Kr I total ion chromatogram (bottom) of the Curie-point (610 °C) pyrolysate of beech MWL. The time scale on the upper trace is indicated by the retention times of the C_{12}–C_{23} *n*-alkanes. The time scales of the two PI chromatograms are in seconds.

that differences in pyrolysis conditions are present, which might be due to the different carrier gases used.

However, the photoionization data clearly show that the relative response to the various compounds depends strongly on the ionizing energy (Table I). It is interesting to note that the Kr I relative response to those methoxyphenols which have an aldehyde, vinyl, or propenyl group at the 4-position is stronger than the Ar I response, whereas the Kr I relative response to acetyl, allyl, and propenol substituted methoxyphenols is lower. It seems that compounds that have the ability of conjugation in the side chain are more easily photoionized than compounds without this feature.

Deconvolution of Py–MS Peaks. Returning to the cumulative spectra in Figure 2, it is now possible to determine the contributions of the various pyrolysis products to these mass spectral fingerprints. From Table I it is clear that almost every nominal mass peak in the fingerprints originates from more than one compound, whereas the relative contributions of the compounds depend strongly on the ionizing energy. For instance, in the Ar I fingerprint mass 124 for the major part originates from the $(M - 56)^+$ fragment of coniferyl alcohol, whereas only 25% is due to the guaiacol. In the Kr I spectrum however mass 124 is almost solely due to the guaiacol, since the Kr I light hardly induces any fragmentation. Mass 180 in the Ar I spectrum represents mainly coniferyl alcohol, with a 15% contribution of syringyl–ethene, but in the Kr I spectrum almost 30% corresponds to syringyl–ethene.

These observations are of great importance for pyrolysis–mass spectrometry, where it is general practice to interpret

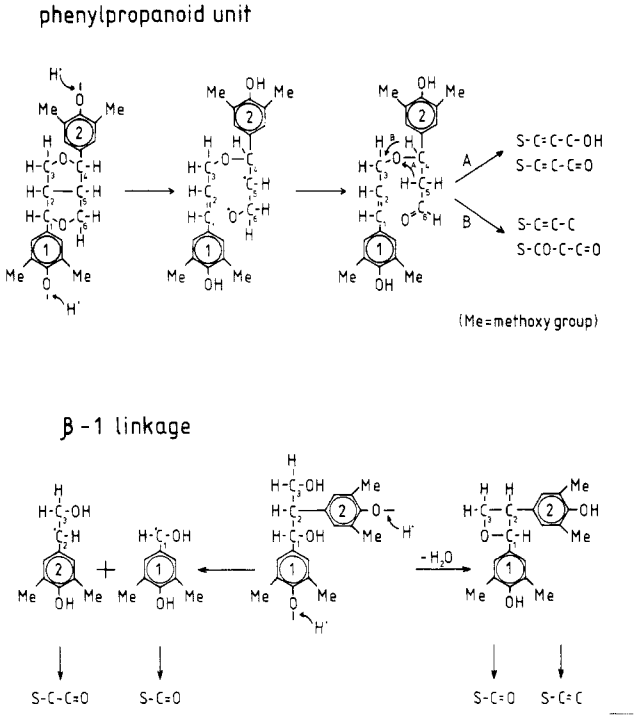

Figure 4. Proposed thermal degradation scheme for two major structural elements in beech lignin, which explains the major pyrolysis products found in the MWL pyrolysate.

Py–MS data chemically by comparison of unknown spectra with those of standards (*2*). The photoionization data show that this practice is not without bias. In comparative work with standards, it is not possible to distinguish different compounds which show up at the same nominal masses in the spectrum. Thus, a reliable chemical interpretation has to be based on the identification of the individual pyrolysate components and the determination of their relative contributions to the fingerprint. Our Py–GC–PIMS method fulfills this requirement, combining the possibility of pyrolysis product identification (Py–GC–MS mode), with the option of a highly condensed form of data representation in one mass spectral fingerprint (Py–MS mode).

CONCLUSIONS

Curie-point pyrolysis–gas chromatography coupled to photoionization mass spectrometry is a promising technique for the analysis and fingerprinting of biopolymer materials. When applied to the determination of lignin, the major pyrolysis products can be related to structural elements in the macromolecule. The pyrolysate provides a good representation of the degree of methoxylation since the pyrolytic depolymerization method applied here leaves the syringyl and guaiacyl units intact.

Photoionization offers the possibility of choosing different stable ionization energies. Ar I mass spectra contain enough structural information to allow identification of the organic compounds. The Ar I Py–MS fingerprints resemble the 15-eV EI Py–MS fingerprints, which enables a direct comparison. Kr I light is most suitable for fingerprinting purposes, since it yields almost only molecular ions.

The strong variations in response and degree of fragmentation with ionizing energy, together with potential mass spectral interferences, will make it difficult to abstract reliable chemical information from low-energy pyrolysis mass spectra alone. Pyrolysis mass spectral fingerprints remain useful for classification of biomaterials such as lignins.

The method described here enables the chemical interpretation of mass spectral fingerprints by tracing back all fingerprint information to the respective contributions of the

individual pyrolysis products.

ACKNOWLEDGMENT

We thank N. M. M. Nibbering for his valuable comments on the paper.

Registry No. MWL, 8068-00-6.

LITERATURE CITED

(1) Irwin, W. J. *Analytical Pyrolysis, a Comprehensive Guide*; Marcel Dekker: New York, 1982; pp 1-578.
(2) Meuzelaar, H. L. C.; Haverkamp, J.; Hileman, F. D. *Pyrolysis Mass Spectrometry of Recent and Fossil Materials*; Elsevier: Amsterdam, 1982; pp 1-293.
(3) Boon, J. J.; Tom, A.; Brandt, B.; Eijkel, G. B.; Kistemaker, P. G.; Notten, F. J. W.; Mikx, F. H. M. *Anal. Chim. Acta* **1984**, *163*, 193-205.
(4) Meuzelaar, H. L. C.; Windig, W.; Harper, A. M.; Huff, S. M.; McClennen, W. H. Richards, J. M. *Science* **1984**, *226*, 268-274.
(5) Vallis, L. V.; MacFie, H. J.; Gutteridge, C. S. *Anal. Chem.* **1985**, *57*, 704-709.
(6) Meuzelaar, H. L. C.; Kistemaker, P. G.; Eshuis, W.; Boerboom, A. J. H. In *Advances in Mass Spectrometry*; Daley, N. R., Ed.; Heyden: London, 1978; Vol. 7B, pp 1452-1456.
(7) Meuzelaar H. L. C.; Huff, S. M. *J. Anal. Appl. Pyrolysis* **1981**, *3*, 111-129.
(8) Whitehouse, M. J.; Boon, J. J.; Bracewell, J. M.; Gutteridge, C. S.; Pidduck, A. J.; Puckey, D. J. *J. Anal. Appl. Pyrolysis* **1985**, *8*, 515-533.
(9) Genuit, W.; Boon, J. J. *J. Anal. Appl. Pyrolysis* **1985**, *8*, 25-40.
(10) Geltman, S. *Phys. Rev.* **1956**, *102*, 171-179.
(11) Washida, N.; Akimoto, H.; Tagaki, H.; Okuda, M. *Anal. Chem.* **1978**, *50*, 910-915.
(12) Tagaki, H.; Washida, N.; Akimoto, H.; Okuda, M. *Anal. Chem.* **1981**, *53*, 175-179.
(13) Sarkanen, K. V.; Ludwig, C. H. *Lignins*; Wiley: New York, 1971; pp 1-916.
(14) Freudenberg, K. *Holzforschung* **1964**, *18*, 3-9.
(15) Adler, E. *Wood Sci. Technol.* **1977**, *11*, 169-218.
(16) Nimz, H. H. *Angew. Chem., Int. Ed. Engl.* **1974**, *13*, 313-321.
(17) Kratzl, K.; Czepel, H.; Gratzl, J. *Holz Roh.-Werkst.* **1965**, *23*, 237-240.
(18) Bracewell, J. M.; Robertson, G. W.; Williams, B. L. *J. Anal. Appl. Pyrolysis* **1980**, *2*, 53-62.
(19) Schenck, P. A.; de Leeuw, J. W.; Viets, T. C.; Haverkamp, J. In *Petroleum Geochemistry and Exploration of Europe*; Brooks, J., Ed.; Blackwell Scientific Publication: Oxford; 1983; pp 267-274.
(20) Martin, F.; Saiz-Jimenez, C.; Gonzalez-Vila, F. J. *Holzforschung* **1979**, *33*, 210-212.
(21) Saiz-Jimenez, C.; de Leeuw, J. W. *Org. Geochem.* **1984**, *6*, 417-423.
(22) Obst, J. R. *J. Wood Chem. Technol.* **1983**, *3*, 377-397.
(23) Boon, J. J.; Pouwels, A. D.; Eijkel, G. B. *Trans. Biochem. Soc.* **1986**, *15*, 170-174.
(24) Genuit, W.; Chen He-Neng; Boerboom, A. J. H.; Los, J. *Int. J. Mass Spectrom. Ion Phys.* **1983**, *51*, 207-213.
(25) Björkman, A. *Sven. Papperstidn.* **1956**, *59*, 477-485.
(26) Faix, O.; Schweers, W. *Holzforschung* **1973**, *27*, 224-229.
(27) Cramers, C. A.; Scherpenzeel, G. J.; P. A.. Leclercq, P. A. *J. Chromatogr.* **1981**, *203*, 207-216.

RECEIVED for review May 16, 1986. Accepted September 30, 1986. This work is part of the research program of the Dutch Foundation for Fundamental Research on Matter (FOM) and was made possible by financial support from the Dutch Foundation for Technical Research (STW).

Quantitative Analysis of Quartz and Cristobalite in Bentonite Clay Based Products by X-ray Diffraction

J. Robert Carter,* Mark T. Hatcher, and Larry Di Carlo

NL Chemicals/NL Industries, Inc., P.O. Box 700, Hightstown, New Jersey 08520

Quartz and cristobalite in beneficiated bentonite clay and organoclay materials have been quantitatively determined by X-ray diffraction. An internal standard method and a mass absorption coefficient correction method were employed to compensate for sample absorption effects. The lower limit of quantitation for quartz and cristobalite in these types of materials is estimated to be 0.01 wt % and 0.03 wt %, respectively. Absolute errors at the 95% confidence level are estimated to be ±0.20% quartz and ±0.35% cristobalite for the internal standard method and ±0.12% quartz and ±0.18% cristobalite for the mass absorption coefficient correction method. A procedure is also described that utilizes the mass absorption coefficient measurement determined by X-ray fluorescence to correct quartz diffraction line intensities in bentonite clays containing high levels of impurities. These methods were successfully employed to monitor the quartz balance of a clay deganguing process in a plant environment and to quantify quartz and cristobalite in commercially available organoclay rheological additives.

With the advent of "right to know" legislation, there is a need to monitor various impurities normally associated with clay and organoclay rheological additives. In particular, there has been considerable interest in monitoring the levels of total quartz and cristobalite in clay-based products since a potential hazard may exist from exposure to dusts containing respirable crystalline silica (*1*). Numerous methods of analyzing quartz have been reported in the literature, for instance, infrared spectroscopy (*2*), wet chemical analysis (*3*, *4*), and differential thermal analysis (*5*). Each of these methods suffers from drawbacks, such as nonspecificity, the lack of sensitivity at low levels, or poor reproducibility.

Since X-ray diffraction is highly specific and can readily distinguish between silica polymorphs, it was decided to use this technique to quantify both cristobalite and quartz. This article describes XRD methods for analyzing cristobalite and/or quartz in crude bentonite clay, refined bentonite clay, and commercial organoclay rheological additive products. The developed standard version of the XRD method illustrates the use of external standard calibration curves and two different techniques in correcting diffraction intensities for matrix effects. Corrections are necessary since variations in chemical composition do occur that can significantly affect the strength of the quartz and cristobalite diffraction intensities. The techniques consist of determining the mass absorption coefficient of each sample with a separate X-ray fluorescence measurement or employing LiF as an internal standard. Special cases where the intensity correction is unnecessary are also discussed.

Clays are natural products and typically contain feldspar, illite, gypsum, zeolite, and calcite in addition to quartz and cristobalite. When present in significant amounts, some of these minerals can contribute errors in the analysis for quartz

0003-2700/87/0359-0513$01.50/0